Available online at www.sciencedirect.com

SCIENCE DIRECT

Powder Technology 161 (2006) 22 – 31

POWDER TECHNOLOGY

www.elsevier.com/locate/powtec

Experimental study of oblique impacts with initial spin

H. Dong *, M.H. Moys

School of Process and Materials Engineering, University of the Witwatersrand, Private Bag 3, Johannesburg, WITS 2050, South Africa

Received 15 November 2004; accepted 16 May 2005
Available online 22 July 2005

Abstract

An experiment to measure the properties of the impacts between of a 44.5 mm steel ball and a steel flat surface is reported. The apparatus can release the ball with and without initial spin. The steel target can be inclined 0–60°. The impact event is recorded with a digital video camera. The video analysis is computer based and all the distortions of image are calibrated. The impact properties measured are expressed as coefficient of normal restitution e_n, coefficient of tangential restitution e_t, impulse ratio or dynamic coefficient of friction f, angular velocity, and rebound angle of the contact point. It is found that the measurement of oblique impact without initial spin shows close agreement with recent published results and complies with rigid body theory. However, the experimental results of oblique impact with pre-impact spin do not agree to the collision models in rolling or micro-slip regime in particular.

Keywords: Impact; Collision; Coefficient of restitution; Angular velocity; Video processing; Image analysis

1. Introduction

Impacts and collisions are ubiquitous, e.g. during galactic evolution, avalanches, ball games, and many other industrial operations handling and processing granular materials, such as chemical, pharmaceutical, agricultural, and mining industries. The classical approach to impact was furnished by Newton with the notion of the coefficient of restitution e in his first book, "Philosophiae Naturalis Principia Mathematica" (1686). Newton's law of impact states that the speed of rebound is proportional to the speed of approach, both taken normal to the impact plane, the constant of proportionality being the coefficient of restitution, $e=v_n^+/v_n^-$. This is the only parameter needed to describe collinear impacts and is still widely employed. However, this approach ignores the details of transient force and displacement during the impact process. Hertz presented his theory of elasticity, which deals with the relationship of the static contact force and the relative approach, $F_n=k_n\alpha^{3/2}$.

The Hertz theory is restricted to frictionless surfaces of perfect elasticity. For oblique impact of frictional solids, the frictional force will reduce the tangential velocity of the mass center and change the angular velocity of the impacting bodies. The pioneering work to formulate the tangential force under normal load was done by Mindlin and Deresiewicz [1]. The magnitude and direction of tangential force is described according to the mode of motion of the contact patch—sliding or rolling. Mindlin and Deresiewicz take into account the loading history of normal and tangential forces to determine the current tangential force. Maw et al. [2] argued that if the distribution of tangential displacement (or traction) would be approximated by a suitable series function, the amount of information carried through the procedure would be independent of the number of time steps used. A numerical method was developed to identify the status of motion in tangential direction [3]. If the non-dimensional rebound angle, ψ_2, is positive, where the impact angle is greater than 30°, the impacts comply with the rigid body theory

* Corresponding author. Tel.: +27 11 7177570; fax: +27 11 4031471.
E-mail address: hongjundong@yahoo.com (H. Dong).

0032-5910/$ - see front matter © 2005 Elsevier B.V. All rights reserved.
doi:10.1016/j.powtec.2005.05.046

(sliding); if the non-dimensional rebound angle is negative, tangential compliance comes into play (rolling or sticking, impact angle less than 30°). This method requires only two parameters to fully describe an impact event, normal coefficient of restitution e and coefficient of friction μ but three parameters (Possion's ratio v, shear stiffness and friction coefficient μ) are needed to calculate the two non-dimensional angles ψ_1 and ψ_2. A simplified model was used by Foster et al. [4] and Lorenz et al. [5] to get rid of the three parameters in the definition of impact and rebound angles and the results are comparably accurate. This is a three constant coefficients model [6]. The coefficients are normal coefficient of restitution e for normal movement, coefficient of friction μ for sliding tangential movement and tangential coefficient of restitution β for rolling or sticking tangential movement. It is believed that the sliding and rolling are mutual exclusive. This is different from Maw's model [2] which allows the contact point to slide at the start of the impact and then its velocity may reach zero during the impact under the influence of opposing frictional force, i.e. sliding will give way to rolling. Once rolling is established, it will persistent to the end of the impact.

Particular effort was invested in the measurement of rotational velocity in experiments carried out to validate the models for oblique impacts. Maw et al. [3] used a strobe to measure the trajectories and rotation of steel and rubber pucks colliding with blocks of the same material, confirming the general form of their two non-dimensional impact-rebound angles model. Gorham and Kharaz [7] and Kharaz et al. [8] used a strobe and single-frame digital camera to measure the speed, angle and rotation before and after impact of a 5 mm aluminium oxide ball impacting a 26 mm thick soda lime float glass (fully elastic) and a 25 mm aluminium alloy anvil (some plastic deformation). This accurate and reproducible result showed very close agreement with Maw's model. Foester et al. [4] and Lorenz et al. [5] used a strobe to characterize the collisions of ball–ball and ball–wall. Their experiments substantiated Walton's three constant coefficients impact model. Labous et al. [9] studied the collision properties of 6.35–25.4 mm nylon spheres with a high speed video camera at a range of normal impact velocity 0.4–60 m/s. The surfaces of spheres were marked with dots to measure their orientation. Their results were compared to Walton's model with satisfactory agreement.

It should be noted that there is no initial spin in all the previous impact tests to the best of our knowledge. In this paper the results of impact of a steel ball with initial spin impacting a chrome steel block is presented. An emphasis is placed on the effect of initial spin on the rebound behaviour. This is an extension of [10] where the behaviour of normal impact and oblique impact without initial spin was investigated with a digital camera at a resolution of 320×240 pixels. This resolution is not adequate for impacts with initial spin. A digital video camera is employed here to record the impact process at a resolution of 720×576 pixels. The results obtained confirmed the rigid body theory for impact without initial spin. However the models based on rigid body theory are not applicable to the impact with initial spin.

2. Experiment method

A schematic set-up of all the equipment used in the experiment is shown in Fig. 1. It has the flexibility to release the ball with or without initial spin. It consists of four parts. (i) A massive table made of steel with a surface of 500×900 mm that can be inclined from zero to 60°, which is indicated by a protractor. On the top of the table is a 74 kg steel block of $362 \times 586 \times 58$ mm. It actually is a piece of liner for grinding mill in a power station. (ii) Ball releasing system. A 44.45 mm diameter ball (358.35 g) is held to a nozzle by vacuum created by a vacuum pump. A 2 mm wide paper band is stuck on the equator of the ball to indicate its orientation for the measurement of angular velocity. To release the ball, the vacuum in the hose is removed by switching off the vacuum pump and switching on the air valve (not shown in the picture) in the hose near the pump to let the air in. The nozzle can be moved horizontally or vertically as indicated. (iii) A digital video camera is put 1.6 m away from the object plane. (iv) An image processing system. The impact event is recorded on a Mini DV tape that is then transferred into a PC as AVI format video clips. The video clips are then decomposed into individual frames with software (Bink and Smacker). Images of even lines, odd lines or a blend of both can be extracted. In the blended mode, the images of the ball are recorded at 50 frames per second (fps). A sequence of frames is shown in Fig. 2, which is further analyzed using a professional image-processing package, OPTIMAS. It can analyze points, lines and areas. A calibration procedure has been carried out to eliminate the distortions caused by illumination, perspective, and lenses that were detailed in Dong and Moys [11]. The digitized result of Fig. 2 is presented in Fig. 3.

To release the ball with initial spin, the ball is wrapped with a strip of paper 40 cm long from a height of 90 cm to the impact point. The ball will unwrap itself under gravity. At the end of unwrapping (there still is one layer of paper around the ball) the energy balance is

$$mgh = \frac{1}{2}mv^2 + \frac{1}{2}I\omega^2 \tag{1}$$

$$I = \frac{2}{5}mr^2 \tag{2}$$

If there is no slip while the ball unwraps itself, a relationship between linear velocity and angular velocity holds,

$$v = r\omega \tag{3}$$

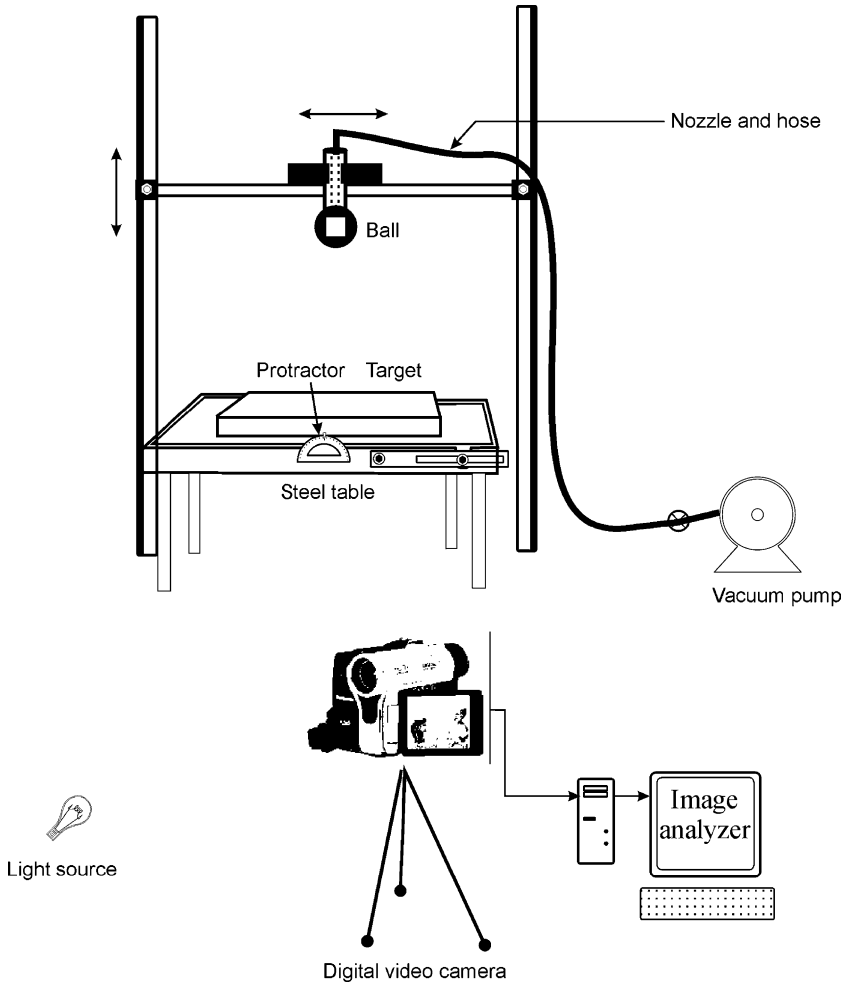

Fig. 1. The experimental set-up (not to scale).

The final angular velocity is obtained from (1)–(3)

$$\omega = \frac{\sqrt{\frac{10}{7}gh}}{r} = 82.08 \text{ rad/s} \quad (4)$$

where h is the unwrapping length, $h = 0.4 - (2\pi + 1)r = 0.238$ m. This is the maximum angular velocity the ball can reach.

3. Oblique impact without initial spin

In this section, the ball is dropped on a steel target that is inclined from 0 to 60°. The drop height is 90 cm corresponding to an impact velocity of 4.2 m/s. The original data obtained from video analysis is (θ, $\omega^-=0$, ω^+, $v_x^-=0$, v_y^-, v_x^+, v_y^+) as shown in Fig. 4. The velocities before and after impact are decomposed into normal and tangential components at the impact point. The final measurement are (θ, ω^+, v_n^-, v_t^-, v_n^+, v_t^+) from which the coefficient of tangential restitution is obtained:

$$e_t = \frac{v_t^+}{v_t^-} \quad (5)$$

It is important to point out that the velocities in Eq. (5) are measured at the center of mass that is same as [12], not at the contact point. The velocity at the contact point has been used to define the coefficient of tangential restitution β [4,9]. The velocity at the contact point is defined below and will be used to discuss sliding later.

$$V_{t,CP}^+ = v_t^+ - r\omega^+ = v_x^+\cos\theta + v_y^+\sin\theta - r\omega^+ \quad (6)$$

Note that when the ball is released without spin $V_{t,CP}^- = v_t^-$. Another parameter, impulse ratio, f, is useful in relating e_t and e_n. It is defined as the ratio of the tangential impulse P_t to the normal impulse P_n during collision.

$$f = \frac{P_t}{P_n} = \frac{v_t^+ - v_t^-}{v_n^- - v_n^+} = \frac{1 - e_t}{1 + e_n}\tan\theta \quad (7)$$

If we assume the tangential force $F_t = \mu F_n$ in the process of impact (i.e., slipping occurs throughout impact), $f = \frac{P_t}{P_n} = \frac{\int F_t dt}{\int F_n dt} = \frac{\int \mu F_n dt}{\int F_n dt} = \frac{\mu \int F_n dt}{\int F_n dt} = \mu$ (true only if μ is constant). So f is sometimes called dynamic coefficient of friction [13]. However, because this assumption is not always true, it is better to term it impulse ratio.

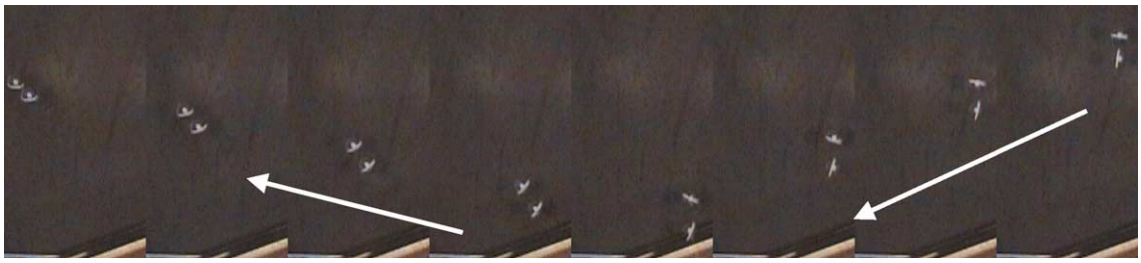

Fig. 2. A sequence of frames extracted from a video clip. The background is a black sheet.

3.1. Coefficients of normal and tangential restitution, impulse ratio tangential to normal

Fig. 5 shows the results of oblique impacts of a 44.5 mm steel ball on a steel liner in terms of e_t, e_n, and f. The coefficient of normal restitution e_n is constant with a value of 0.90 ± 0.02 at any inclination from 0 to 60° where the normal component velocity ranges from 4.2 m/s at 0° to 2.0 m/s at 60° target inclination That is not big enough to make a notable difference in normal coefficient of restitution. Generally speaking, normal restitution coefficient will decrease with the increase of impact velocity as observed by Labous et al. [9]. A range of models has been proposed to describe the coefficient of restitution as a function of impact velocity [14–16].

The coefficient of tangential restitution e_t in Fig. 5 is always less than the coefficient of normal restitution. It increases with plate inclination in excellent agreement with [12] (Fig. 8) in trend and value. A detailed study [7] of elastic impacts of 5 mm aluminum oxide spheres on a glass anvil tilting from 2° to 85° reveals that e_t reaches a minimum of 0.6 at an angle close to 20° and approaches a value of 1 only for glancing incidence. The scatter in e_t values is ascribed to the local variations in surface conditions. The scatter in e_n is not as much as that e_t because the measurement of e_n does not depend so much on surface properties.

The impulse ratio f increases from slightly bigger than zero to a limiting constant value of 0.103 on average since 20° incidence. This transition in impulse ratio indicates a change in behaviors of the ball on the surface in tangential direction. It either rolls at low angles (<20° here) or slides at more oblique angles (>20° here). It is reasonable to regard impulse ratio f as dynamic coefficient of friction at high impact angles. According to classical rigid body theory, it is easy to derive a relationship among e_t, e_n, and μ when the ball slides [12]:

$$e_t = 1 - \mu(1 + e_n)\cot\theta \tag{8}$$

Fig. 6 shows e_t values in the sliding regime from Fig. 5 plotted against $(1+e_n)\cot\theta$. The linear regression equation that best fits the measurements is inserted into Fig. 6 giving a coefficient of friction $\mu = 0.091$. This is comparable to the average impulse ratio 0.103. The point for 10° in Fig. 6 deviates greatly from the straight line. From Figs. 5 and 6 it can be concluded that without initial spin the

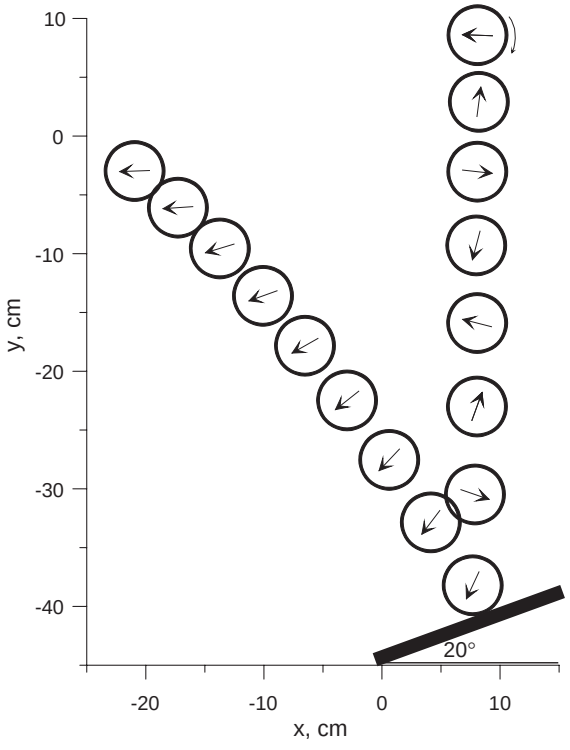

Fig. 3. The position and orientation of the ball by image analysis of Fig. 2.

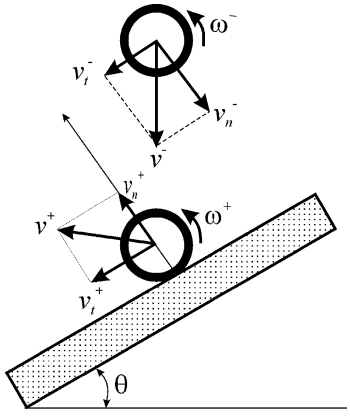

Fig. 4. The impact of a ball on an oblique surface. Top, before impact; bottom, the ball leaving the surface.

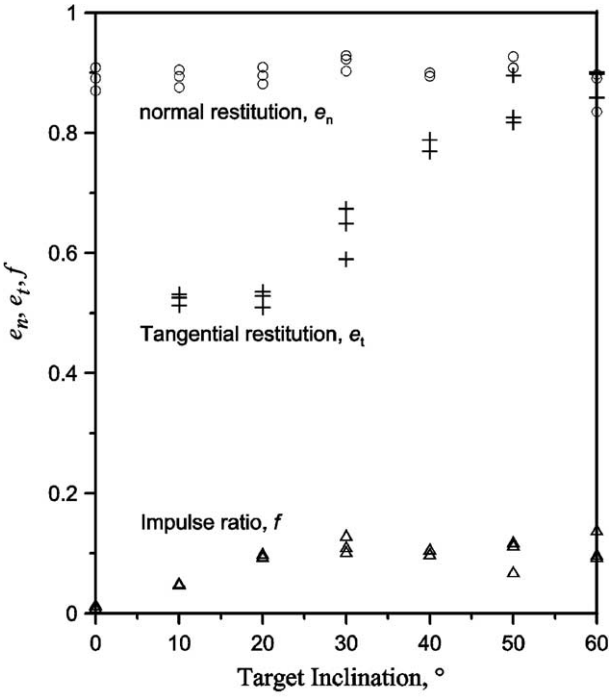

Fig. 5. Coefficient of restitution, normal and tangential, and impulse ratio tangential to normal of a steel ball impacting steel liner. No initial spin, fall height=0.90 m.

44.5 mm steel ball slides on the chrome-steel surface when the impact angle >20°; it rolls or micro-slips when the impact angle <20°.

3.2. Angular velocity without initial spin

Fig. 7 presents the measurements of angular velocity after impact from 10° to 60° at an incremental of 10° as filled circles. The open triangles co-plotted are rotation results from [7] of 5 mm Al_2O_3 balls impacting a 26 mm thick soda glass anvil. It can be seen that the rotation

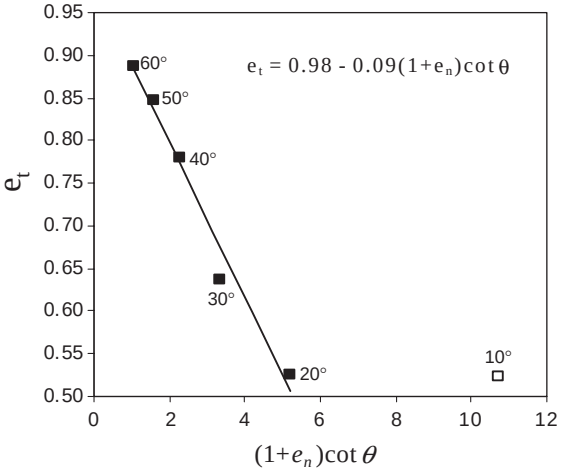

Fig. 6. Measurement e_i plotted against $(1+e_i)\cot\theta$. The equation for the straight line is inserted in the plot.

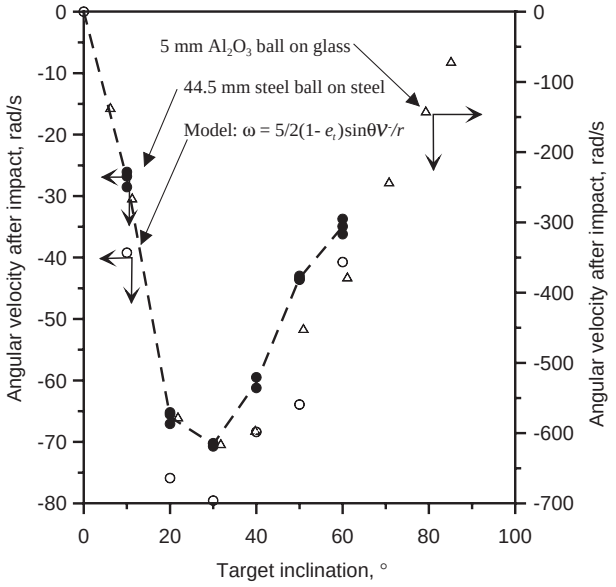

Fig. 7. Angular velocity after impact without pre-spin.

reaches zero at the two extreme inclination angles. For oblique elastic impact of a ball on a flat surface without initial spin, the angular velocity after impact acquired from tangential impulse in terms of the tangential coefficient of restitution according to rigid body theory is given [7]:

$$\omega^+ = \frac{5}{2}(1 - e_t)\sin\theta\frac{v^-}{r} \tag{9}$$

Fig. 7 also shows the value of angular velocity (as open circles) calculated from direct measurement of e_t using Eq. (9). Gorham's rotation velocity is about nine times higher than our measurement at every angle. This is because the angular velocity is inversely proportional to the diameter of ball and their balls are nine times smaller than ours (the impact velocities, v^-, are also comparable. Gorham's drop height is 820 mm, 3.8 m/s and our drop height is 900 mm, 4.2 m/s). It is clear that there is a close agreement among the three sets of data. This agreement confirms the applicability of the assumptions of rigid body theory for the elastic impact between a ball and a flat surface. The maximum angular velocity at 30° coincides with the angle of transition between rolling and sliding in Fig. 5. It is

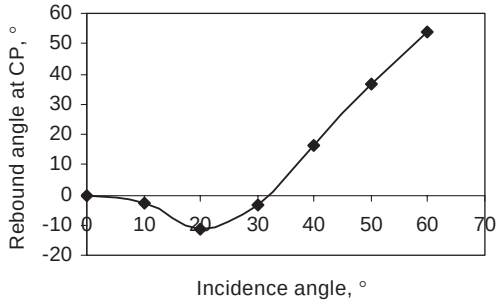

Fig. 8. Rebound angle at contact point against incidence angle of mass center. No pre-spin.

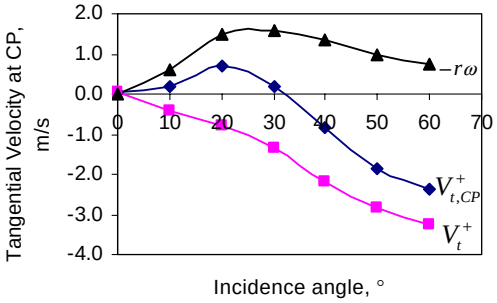

Fig. 9. Tangential velocity at the contact point.

important to point out that this model does not apply to non-elastic impact. An oblique impact test of a steel ball on a rubber surface showed that the rebound angular velocity increases monotonically with the target inclination angle. No minimum value is observed in post-impact spin as in Fig. 7 [10].

3.3. Rebound angle at contact point without initial spin

The rebound angle at contact point, θ_r, is defined in such a way that it takes a positive value when the rebound trace of the contact point lies in the opposite side to the incidence trace with regard to the normal line of the contact surface. If both the incidence and rebound traces are on the same side, the rebound angle is negative.

$$\theta_r = a\tan\frac{-V^+_{t,CP}}{V^-_{n,CP}} \tag{10}$$

$$V^+_{t,CP} = v^+_t - r\omega^+ = v^+_x\cos\theta + v^+_y\sin\theta - r\omega^+ \tag{11}$$

At the contact point, $V^+_{n,Cp}=v^+_n$. The calculated values of θ_r and $V^+_{t,CP}$ using Eqs. (10) and (11) are plotted in Figs. 8 and 9. The rebound angle versus incidence angle displays a similar form to results presented as the non-dimensional rebound angle versus incidence [3,7] and the simplified version of non-dimensional rebound and incidence angles [4]. Maw et al. [3] and Gorham and Kharaz [7] believe that (i) when the rebound angle is positive the impact ends in a state of gross slip (sliding). A sliding coefficient of friction can be derived; (ii) when the rebound angle is negative the impact ends in a state of rolling (sticking) at low incidence angles (<5°) and micro-slip at slightly higher incidence angles (10–30°). This result is comparable to that from the impulse ratio in Fig. 5.

Fig. 9 shows the tangential velocity at the contact point and its two components. The curve for $V^+_{t,CP}$ is a mirror image of rebound angle so that they carry the same information as far as rebound direction is concerned. This is due to the minus sign in the definition of θ_r in Eq. (10). $V^+_t=e_t v_i\sin\theta$. It has a negative value because v_i is negative when it is dropped down. The negative value in $V^+_{t,CP}$ is ascribed to tangential compliance by [2,17]. However, the velocity at the center of mass does not change direction as can be seen in Fig. 5 so that e_t is always positive.

4. Oblique impact with initial spin

4.1. The direction of pre-impact spin

Fig. 10 shows how a pre-impact spin is produced. If the paper strip wrapping the ball forms a letter b as illustrated in Fig. 10(a), the ball will spin forward on the flat surface. This kind of spin is termed forward spin or clockwise spin. The angular velocity of forward spin is positive according to right hand law; if the paper strip forms a letter d with the ball as illustrated in Fig. 10(b), it is called backward spin or anticlockwise spin. The angular velocity will have a negative sign. As shown in Fig. 7, the ball will spin backwards after impact when it is dropped without initial spin. This section will investigate the effect of pre-impact spin on the rebound behavior.

4.2. e_t, e_n, and f of impact with clockwise spin

Fig. 11 shows the effect of forward spin in b-type drop on impact parameters e_t, e_n, and f parallel to Fig. 5. (i) The coefficient of restitution e_n is constant at a value of 0.93 ± 0.02, which is nearly the same as e_n without initial spin (0.90 ± 0.02). (ii) The impulse ratio is also constant at 0.09 ± 0.02 over the whole range of target inclination angles investigated that is very close to the value of dynamic coefficient of friction obtained in Figs. 5 and 6. It is implied that the ball slides at the contact point throughout when it is dropped with forward initial spin. This means that forward spin promotes sliding as expected. (iii) It is worth noting that the tangential restitution coefficient is negative when the target inclination $\theta<10°$. It indicates that the center of mass of the ball rebounds on the same side of the normal line as the incidence velocity due to the forward spin. The effect of initial forward spin will be cancelled out with the increase of target inclination that will produce a backward spin as demonstrated in Fig. 7.

4.3. e_t, e_n, and f of impact with anticlockwise spin

Fig. 12 shows the effect of backward spin in d-type drop on impact parameters e_t, e_n, and f. It can be seen that (i) the

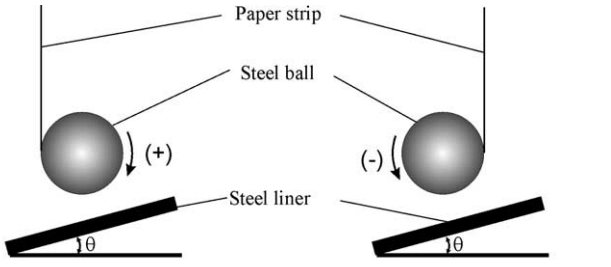

Fig. 10. The direction of pre-impact spin. The sign of angular velocity is determined by right hand law.

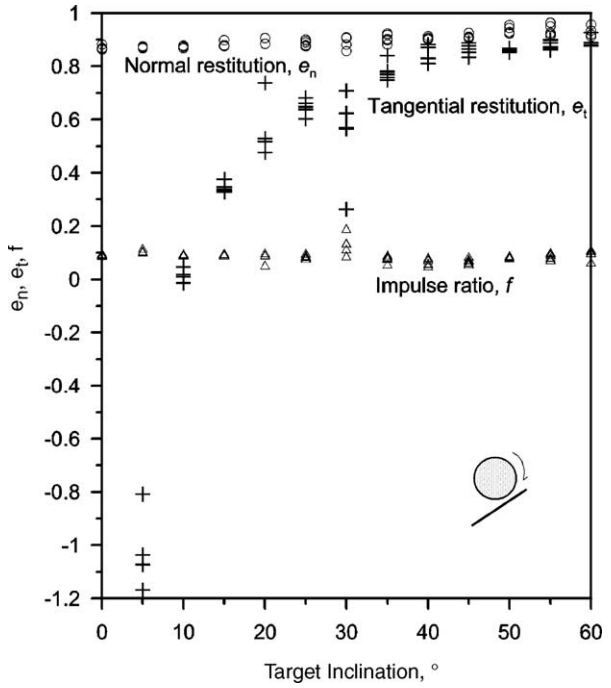

Fig. 11. e_n, e_t, f of impact in b-type drop (+).

coefficient of restitution e_n is constant at a value of 0.86 ± 0.04, which is slightly smaller than e_n without initial spin (0.90 ± 0.02); (ii) the impulse ratio is only constant at 0.11 ± 0.02 when the target inclination angle is bigger than 40°and it is also very close to the value of dynamic coefficient of friction obtained in Figs. 5 and 6. It is implied that the ball slides later at the contact point. The backward pre-spin hinders sliding of the contact point compared with the no pre-spin case; (iii) the tangential restitution coefficient, e_t, approaches positive infinite when the target inclination is close to 0° due to small tangential velocity imparted to the mass center by the initial spin. This is opposite to the situation of forward initial spin.

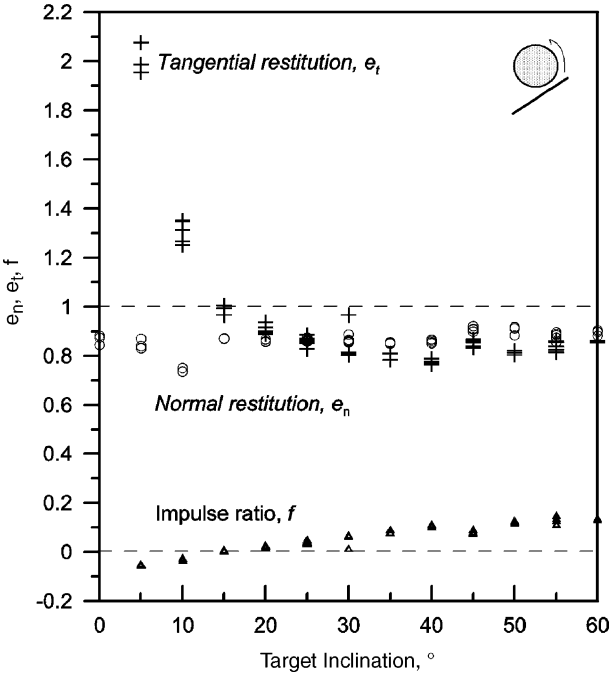

Fig. 12. Coefficient of normal and tangential restitution, and impulse ratio for d-type drop (−).

4.4. Angular velocity with initial spin

Fig. 13 presents the measurements of angular velocity after impact from 0 to 60° at an increment of 5° when the ball is dropped with an pre-spin of about 80 rad/s. The angular velocity after impact without initial spin is also plotted here for convenience of reference. It is important to point out that the model in Eq. (9) is no longer applicable to impact with pre-impact spin for the reason that tangential restitution coefficient e_t has very different values at low angles and similar values at high angles for the two different initial spins. At low impact angles (0–5°), the tangential force dominates the rotation behavior. It brings the initial angular velocity to almost zero. The rotational kinetic energy is converted to tangential kinetic energy. This causes the ball to rebound at 11.4° away from its incidence (also normal) direction as illustrated in Figs. 14 and 15. For the forward spin (clockwise) its initial rotational direction is opposite to the direction of rotation imparted during the impact by the tilted target. Its angular velocity after impact is always smaller than its initial angular velocity due to the dual effect of friction and target inclination. In the backward spin case, the

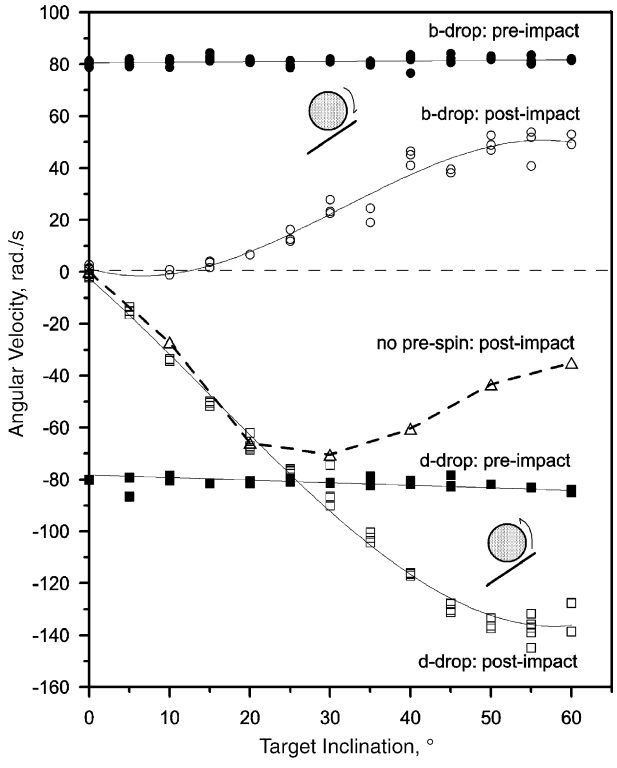

Fig. 13. Angular velocities before and after impact of a 44.5 mm diameter steel ball impacting a flat surface of chrome steel.

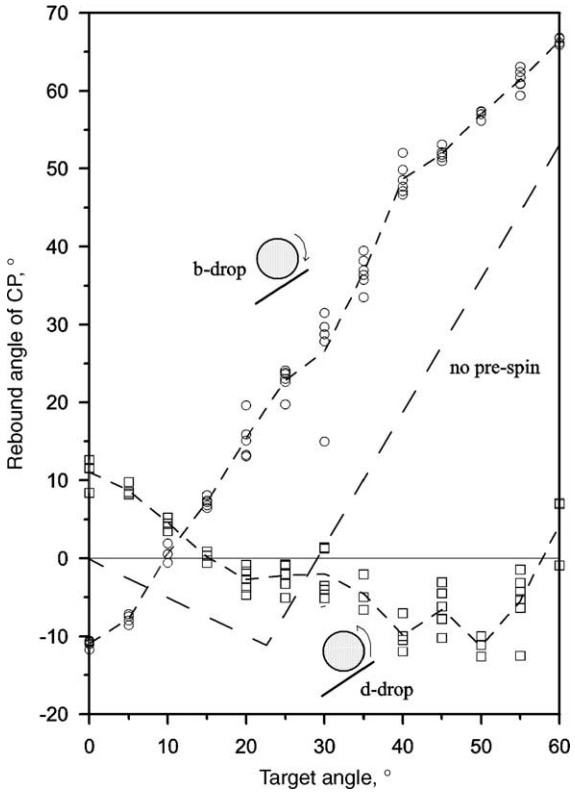

Fig. 14. Rebound angle of CP of the ball dropped with 80 rad/s initial spin.

ball's angular velocity after impact is bigger than its initial velocity because the angular velocity produced by the target has the same direction as the initial angular velocity. In the rolling/sticking regime for the backward initial spin, the angular velocity after impact is nearly the same as that of no initial spin. This implies that the frictional force is small or even zero in rolling regime and the rotational velocity after impact is produced by tangential compliance [3].

4.5. Rebound angle of contact point and the center of mass

The rebound angles at contact point are plotted against the incidence angle in Fig. 14. In the b-type drop (forward spin) case, the rebound angle at contact point follows a straight line with target angle. It has been demonstrated in Fig. 11 that the contact point slides over the whole range of target angles. Its bigger values compared with that for d-drop indicate that it has a higher velocity at contact point than that in d-drop. In d-drop case, the rebound angle is in the range of $-15°<\theta_r<15°$. This means that the velocity at contact point is small. The impulse ratio in Fig. 12 shows the contact point rolls when the target inclination is smaller than 40° and slides thereafter. Theoretically speaking, the velocity of the contact point should be zero when the ball rolls on the contact surface. It is better to say the ball is in a state of micro-slip at the end of impact. The condition for rolling/sticking is difficult to satisfy.

For a ball impacting a plane, it is predicted that $e_t=5/7=0.714$ for rolling to occur ($V^+_{t,CP}=0$ and $\theta_r=0°$) from the following kinematical consideration [8]

$$e_t=\frac{2}{7}e_n\frac{\tan\theta_r}{\tan\theta_i}+\frac{5}{7} \tag{11}$$

However, from the measurement of e_t in Figs. 5, 11 and 12, e_t has a value of 5/7 only at a specific angle of target inclination and the ball is not always in a rolling regime at this condition. $e_t=5/7$ is neither sufficient nor necessary for rolling to occur.

Initial spin also makes the three constant coefficient impact model [6] inapplicable in the rolling regime. For example, the rebound angle versus incidence for the no pre-spin case can be modeled with two straight lines in Fig. 14 as has been done in [4,5]. The slope of the line for the sliding region is the coefficient of friction and the slope of the line for the rolling region is the coefficient of tangential restitution at the contact point β. However, the value of β is not constant for impact with initial spin. It can be positive or negative in both kinds of spin.

The rebound angle of the center of mass of the ball is shown in Fig. 15. At 0° of target inclination, the ball rebounds 11.4° on average to the left of normal when it is dropped with backward initial spin; it rebounds 11.4° to the right of normal with forward initial spin. When the target is horizontal, the rebound angles at mass center are respectively equal to the rebound angles at the contact point (Fig. 14) in the three dropping scenarios because the rebound angular velocity is zero or close to zero at 0° inclination as shown in Fig. 13 where the tangential velocity of the mass

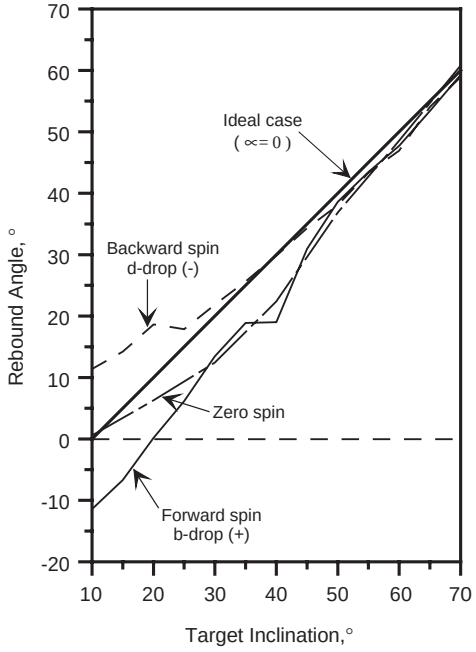

Fig. 15. Incidence and reflection angle of the center of mass of a 44.5 mm steel ball impacting a chrome steel anvil with a 90 cm drop height.

center and the contact point are equal. They begin to deviate since the target is inclined and the ball is imparted an angular velocity after impact. After 40° of target inclination the rebound angles for the three dropping modes converge to ideal rebound angle and the ball slides at the contact surface in all three dropping modes.

5. Conclusions

An experimental procedure has been developed to determine impact parameters of ball impacting a flat surface obliquely. The ball can be released without spin or with initial spin in two directions. The impact event is recorded with a digital video camera at a resolution of 720 by 576 pixels. The position of the center of ball and orientation are measured at the same time using video analysis with a function of calibration of all kinds of image distortions.

The parameters characterizing oblique impact include coefficient of normal restitution e_n, coefficient of tangential restitution e_t, impulse ratio f (or coefficient of friction μ when the ball slides on impact surface), coefficient of tangential restitution of contact point β and rebound angle of contact point θ_r.

Initial spin before impact has a limited effect on the coefficient of normal restitution: $e_n=0.90$ for no pre-spin, 0.93 for forward initial spin 0.86 for backward initial spin. The dynamic coefficient of friction (impulse ratio in sliding regime) of steel ball on chrome steel (28% Cr) surface falls in a range of 0.09–0.11 for all three dropping modes.

Impulse ratio f is a straightforward parameter to determine the mode of motion at the contact point, sliding or rolling. The results of impact without pre-impact spin confirmed the rigid body theory (Figs. 6–8). The results of impact with pre-impact spin did not comply with the rigid body theory (Maw's model and Walton's model). It is found that the rebound angle of the contact point was not necessarily negative for rolling or micro-slip as Maw's model predicted and the tangential coefficient of restitution of contact point is not constant for rolling as Walton's model assumed. It remains a challenge to model the event of elastic impact with initial spin.

List of symbols

CP	contact point
e, e_n	coefficient of normal restitution
e_t	coefficient of tangential restitution
f	impulse ratio normal to tangential during impact or dynamic coefficient of friction
F_n	normal force
I	moment of inertia
K_n	normal spring constant
m	mass of the ball
r	radius of ball
v^-, v_i	velocities of the ball before impact
v^+	velocity of the ball after impact
v_x^-, v_x^+	x component velocity of the ball before and after impact
v_y^-, v_y^+	y component velocity of the ball before and after impact
v_n^+, v_t^+	normal and tangential velocity after impact
v_n^-, v_t^-	normal and tangential velocity before impact
V_{CP}^-	velocity at contact point before impact
$V_{t,CP}^+$	velocity at contact point after impact
α	normal approach
β	coefficient of tangential restitution of contact point
ω^-, ω^+	angular velocity of the ball before and after impact
θ	angle of target inclination in degree
θ_r	rebound angle of contact point
θ_i	incidence angle of impact
μ	coefficient of friction

Acknowledgements

This research was jointly funded by the University of the Witwatersrand, Johannesburg and Eskom. The donation of the steel liner by Eskom used in this paper is greatly appreciated.

Reference

[1] R.D. Mindlin, H. Deresiewicz, Elastic spheres in contact under varying oblique forces, Journal of Applied Mechanics 20 (1953) 327–344.
[2] N. Maw, J.R. Barber, J.N. Fawcett, The oblique impact of elastic spheres, Wear 31 (1976) 101–114.
[3] N. Maw, J.R. Barber, J.N. Fawcett, The role of elastic tangential compliance in oblique impact, Journal of Lubrication Technology 103 (1981) 74–80.
[4] S.F. Foerster, M.Y. Louge, H. Chang, K. Allia, Measurements of the collision properties of small spheres, Physical Fluids 6 (3) (1994) 1108–1115.
[5] A. Lorenz, C. Tuozzolo, M.Y. Louge, Measurements of impact properties of small, nearly spherical particles, Experimental Mechanics 37 (3) (1997) 292–298.
[6] O.R. Walton, Granular Solid Flow Project, Quarterly Report UCID-20297-88-1, Lawrence Livermore National Laboratory (1988).
[7] D.A. Gorham, A.H. Kharaz, The measurement of particle rebound characteristics, Powder Technology 112 (3) (2000) 193–202.
[8] A.H. Kharaz, D.A. Gorham, A.D. Salman, An experimental study of the elastic rebound of spheres, Powder Technology 120 (2001) 281–291.
[9] L. Labous, A.D. Rosato, R.N. Dave, Measurements of collisional properties of spheres using high-speed video analysis, Physical Review E 56 (5) (1997) 5717–5725.
[10] H. Dong, M.H. Moys, Measurement of impact behaviour between balls and walls in grinding mills, Minerals Engineering 16 (2003) 543–550.
[11] H. Dong, M.H. Moys, A technique to measure velocities of a ball moving in a tumbling mill and its applications, Minerals Engineering 14 (8) (2001) 841–850.
[12] R. Sondergaard, K. Chaney, C.E. Brennen, Measurements of solid spheres bouncing off flat plate, Journal of Applied Mechanics 57 (1990) 694–699.

[13] W. Goldsmith, Impact: The Theory and Physical Behavior of Colliding Solids, First ed., Edward Arnold (Publishers) Ltd., London, 1960, p. 379.
[14] K.L. Johnson, Contact Mechanics, 1st ed., Cambridge University Press, Cambridge, 1985, p. 452.
[15] R. Ramirez, T. Poschel, N.V. Brilliantov, T. Schwager, Coefficient of restitution of colliding viscoelastic spheres, Physical Review E 60 (4) (1999) 4465–4472.
[16] C. Thornton, Coefficient of restitution for collinear collisions of elastic-perfect plastic spheres, Journal of Applied Mechanics 64 (2) (1997) 383–386.
[17] R.D. Mindlin, Compliance of elastic bodies in contact, Journal of Applied Mechanics 16 (1949 (September)) 259–268.